



ELSEVIER

Contents lists available at ScienceDirect

Chinese Chemical Letters

journal homepage: www.elsevier.com/locate/cclet

Communication

Construction and regulation of imidazo[1,5-*a*]pyridines with AIE characteristics *via* iodine mediated Csp²-H or Csp-H amination

Jun Zhang^{a,1}, Mengyao She^{a,b,1}, Lang Liu^a, Mengdi Liu^a, Zhaohui Wang^a, Hua Liu^a, Wei Sun^a, Xiaogang Liu^c, Ping Liu^a, Shengyong Zhang^a, Jianli Li^{a,*}

^a Ministry of Education Key Laboratory of Synthetic and Natural Functional Molecule Chemistry, College of Chemistry & Materials Science, Northwest University, Xi'an 710127, China

^b Lab of Tissue Engineering, Provincial Key Laboratory of Biotechnology of Shaanxi, Ministry of Education Key Laboratory of Resource Biology and Modern Biotechnology, The College of Life Sciences, Faculty of Life and Health Science, Northwest University, Xi'an 710127, China

^c Fluorescence Research Group, Singapore University of Technology and Design, Singapore 487372, Singapore

ARTICLE INFO

Article history:

Received 21 February 2021

Revised 7 May 2021

Accepted 13 May 2021

Available online xxx

Keywords:

Aggregation-induced emission (AIE)

Imidazo[1,5-*a*]pyridines

Iodine

Bioimaging

Anti-inflammatory

ABSTRACT

The widespread applications of aggregation-induced emission luminogens (AIEgens) inspire the creation of AIEgens with novel structures and functionalities. In this work, we focused on the direct and efficient synthesis of a new type of AIEgens, imidazo[1,5-*a*]pyridine derivatives, *via* iodine mediated cascade oxidative Csp²-H or Csp-H amination route from phenylacetylene or styrenes under mild conditions. The resulted compounds showed excellent AIE characteristics with tunable maximum emissions, attractive bioimaging performance, and potential anti-inflammatory activity, which exert broad application prospects in material, biology, medicine, and other relevant areas.

© 2021 Published by Elsevier B.V. on behalf of Chinese Chemical Society and Institute of Materia Medica, Chinese Academy of Medical Sciences.

Aggregation-induced emission (AIE) phenomenon has drawn considerable attention and experienced rapid development since it was first discovered by Tang and his co-workers in 2001 [1]. The aggregation-induced emission luminogens (AIEgens) are widely applied in biosensors, organic light-emitting diodes, photovoltaic material, and many other areas, displaying remarkable performances [2–5]. Recently, an AIE dot based IgM/IgG antibody kit has been developed and employed in the diagnosis of 2019-nCoV with high sensitivity and detection speed [6]. Although classical tetraphenylethylene derivatives possess excellent optical properties, they are not sufficient to meet the growing demand of modern materials science during the past decade [7–9]. Many efforts have been made to develop new types of AIEgens to achieve desired properties, among them many researchers have demonstrated that introducing heteroatoms into the AIEgen structures could optimize the optical properties due to the participation of lone pair electrons or empty orbits in their electronic structures [10–13].

Many new heterocyclic fluorogens have been successfully developed during the past decades, among which imidazo[1,5-

a]pyridines exhibited intriguing merits of solid-state luminescence, long fluorescence lifetime, and large Stokes shifts, which allowed them to be employed as the signal moiety to construct fluorescent sensors for the detection of endogenous cell factors such as SO₂, Cu²⁺, cysteine [14–17]. However, their optical properties were still limited by the aggregation caused quenching (ACQ) effect to a certain extent, the construction of imidazo[1,5-*a*]pyridines with excellent AIE characters remains a challenge.

Enhancing the three-dimensional steric hindrance and limiting the intermolecular rotations of fluorophore were widely recognized as effective strategies for suppressing the ACQ effect [18–20]. To date, many strategies including multicomponent reaction, denitrogenative transannulation and cascade Csp³-H amination have substantially improved the construction of imidazo[1,5-*a*]pyridines, but the synthetic method for increasing tridimensional features are still very scarce, and the existing methods were difficult to achieve one-step synthesis. Furthermore, these works were commonly achieved *via* reaction of aldehyde [21,22], nitrile [23,24], benzylamine [25–29], amino acid [30,31], methyl ketone [32] with heteroaryl ketones, alkyl pyridine, and pyridin-2-ylmethyl-amine derivatives, while cyclization of styrene or phenyl derivatives to imidazo[1,5-*a*]pyridine has not yet been reported. Based on the previous works and our long-term interests in the construction of fluorescent molecules [33–35], we hypothesized that

* Corresponding author.

E-mail address: lijianli@nwu.edu.cn (J. Li).

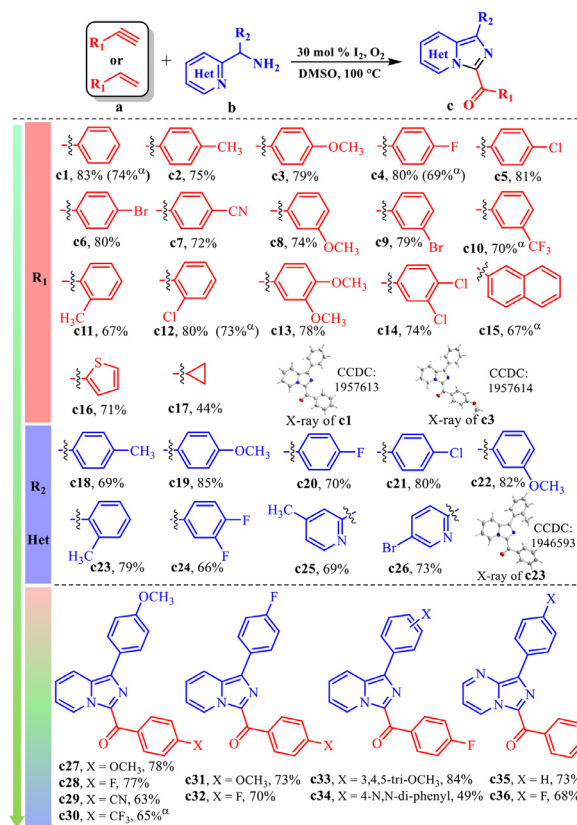
¹ These authors contributed equally to this work.

introducing the carbonyl unit to imidazo[1,5-*a*]pyridines could reduce the ACQ effect caused by the π - π stacking interaction and modulating intermolecular rotations, leading to AIEgens with excellent optical performance (Fig. 1). We further speculated the carbonyl unit could be inserted into the skeleton probably via I_2 -mediated Kornblum oxidation (from phenylacetylene to phenylglyoxal), then going through subsequently cyclization with proper synthons to form benzoyl-imidazo[1,5-*a*]pyridine.

To verify the above hypotheses, an investigation of optimal reaction conditions was conducted using the reaction of phenylacetylene (**a1**) with phenyl(pyridin-2-yl)methanamine (**b1**) as the model (Table S1 in Supporting information). At first, the reaction of **a1** (0.5 mmol) with **b1** (0.5 mmol) was performed in DMSO at 100 °C with the addition of 0.5 equiv. of iodine, while only a trace amount of benzoyl-imidazo[1,5-*a*]pyridine **c1** was detected. Surprisingly, the reaction efficiency was distinctly enhanced when treated with oxidants including $K_2S_2O_8$, TBHP, DTBP, TBPB, and O_2 . With the promotion of O_2 , the mixture smoothly transformed into **c1** with a yield of 42%. Considering the alkylation of pyridine with intermediated α -iodo acetophenone of **a1** may suppress the desired transformation, different acid was introduced into the system to promote the reaction. As expected, the reaction efficiency was significantly improved and gave 68% yield of **c1** in the presence of HCl. With further modulation of the iodine catalyst, solvent and temperature, the reaction achieved a good yield of **c1** up to 83% (Table S1, entry 19). Furthermore, it is surprising that the yield of **c1** could still reach 74% when phenylacetylene was replaced by styrene.

With the optimal conditions, phenylacetylenes with alkyl, alkoxy and halide were successfully screened and transform into the desired products with yields from 75% to 81% (**c2–c6**, **c8**, **c9**), while valuable cyano substituted phenylacetylene is well compatible to giving **c7** with a yield of 72% (Scheme 1). It was notable that the electron-donating groups on the ortho-position of phenylacetylenes would suppress the reaction while the electron-withdrawing group exerted no significant influences on the yields of the desirable products (**c11**, **c12**). Furthermore, poly-substituted phenylacetylenes were also suitable for affording the target compounds (**c13**, **c14**) with satisfactory yields up to 78%. Besides, this new catalytic system is also applicable to hetero and aliphatic substituted alkynes leading to **c16** and **c17** with acceptable yields of 71% and 44%, respectively. Similar to the reaction from styrene to **c1**, other styrene derivatives were also applicable to the current system, leading to corresponding products in good yield such as **c4**, **c10**, **c12** and **c15**. Besides, the substituent group on the benzene ring of R_2 exhibited good compatibility, whether electron-withdrawing or electron-donating (**c18–c24**). The effect of substituents on the pyridine ring was also investigated and exhibited no significant influence on the transformation (**c25**, **c26**). When the substituents on R_1 and R_2 were changed simultaneously, the reaction would still proceed smoothly even for *N,N*-diphenyl substituted substrate (**c27–c34**). Furthermore, the reaction can also be extended to more complicated imidazo[1,5-*a*]pyrimidines in good yields (**c35**, **c36**).

Intriguingly, all the synthesized compounds presented strong solid-state fluorescence under the illumination of 370 nm with large Stokes shifts. To verify the AIE characters and establish the structure-property relationship, 19 compounds with different substitutions were selected to analyze the detailed optical performance (Table 1). The representative compound **c1** emitted weak yellow-green fluorescence at the peak emission wavelengths of 510 nm with a relatively low quantum yield (Φ_f) of 1.6% in THF. Along with the gradually increased water fraction from 0% to 99%, a red-shift of the maximum wavelength to 517 nm and a higher quantum yield (4.2%) was observed (Fig. S23 in Supporting information). The substitution of R_1 , both by electron-withdrawing and



Scheme 1. The extension of the scope of the reaction substrates. Conditions: **a** (0.5 mmol), **b** (0.6 mmol), I_2 (0.1 mmol), and HCl (1 equiv.) were stirred in DMSO with an O_2 balloon at 100 °C. All the yields are isolated yields. ^a Reaction was performed with corresponding styrenes.

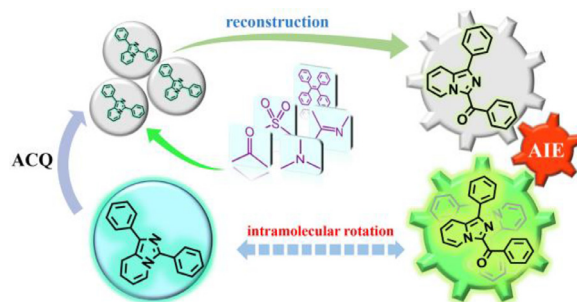


Fig. 1. Proposed imidazo[1,5-*a*]pyridine based AIE dyes by inhibiting the intramolecular rotation.

electron-donating group, would substantially promote the AIE effect of the corresponding products (**c3**, **c4**, **c8** and **c10**) (Figs. S24–S27 in Supporting information). In these compounds, **c10**, the trifluoromethyl substituted compound displayed a more prominent enhancement of quantum yield (0.4% to 6.4%) and bathochromic shift in peak emission wavelengths. Similar effects were also observed when the electronic effect of R_2 was changed (**c19**, **c20** and **c22**) (Figs. S28–S30 in Supporting information). However, the emission and quantum yield did not improve when R_2 was changed to a large and steric group, which may be caused by the inhibited aggregation behaviors (**c23**). Moreover, substituents on the pyridine ring did not exhibit significant promotion of AIE performance (**c25** and **c26**) (Figs. S32 and S33 in Supporting information). Based on these results and previous literature [36,37], the AIE properties of these compounds could be ascribed to the formation of the donor- π -acceptor (D- π -A) structure among R_1 , R_2 , and heterocycle. Thus,

Table 1
The optical properties of selected compounds.

	λ_{ab} ^a (nm)	$\lambda_{em,sol}$ ^b (nm)	$\lambda_{em,agg}$ ^c (nm)	I_a/I_0	Φ_s ^d (%)	Φ_a ^e (%)
c1	376	510	517	2.1	1.6	4.2
c3	400	485	509	4.3	2.9	7.3
c4	408	503	512	20	2.2	6.2
c8	398	511	524	3.6	1.8	5.6
c10	375	513	547	30.3	0.4	6.4
c19	400	468	521	2.9	1.0	6.0
c20	354	533	549	3.0	1.9	5.7
c22	390	512	524	3.6	2.2	5.9
c23	395	504	500	1.8	0.2	1.7
c25	370	465	505	14	0.7	3.4
c26	372	498	511	0.7	2.3	2.0
c27	405	498	529	1.1	6.8	7.7
c28	406	513	540	3.1	1.7	7.1
c29	406	497	554	1.5	1.6	3.3
c30	406	504	569	3.2	4.0	8.2
c31	399	491	528	3.0	1.3	4.5
c32	377	494	527	1.9	2.7	5.1
c33	397	525	550	6.3	3.6	10.9
c34	397	530	558	3.0	6.5	12.6

^a Maximum UV absorption wavelength in THF.

^b Maximum emission wavelength in THF.

^c Maximum emission wavelength in H₂O/THF (99/1, v/v).

^d Absolute quantum yield calculated in THF solution.

^e Absolute quantum yield calculated in H₂O/THF (99/1, v/v).

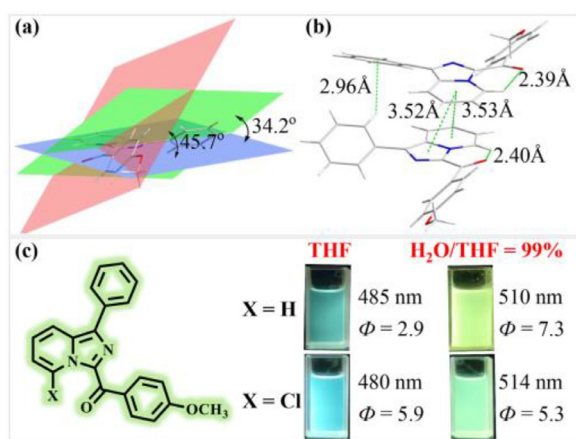


Fig. 2. (a, b) Crystal structures and packing patterns of **c3**. (c) Control experiment to illustrate the effect of the intramolecular hydrogen bond.

the fluorescence regulating effect of synchronously changing R₁ and R₂ were further investigated to generate **c27**–**c34** (Figs. S34–S41 in Supporting information). It is worth noting that when R₁ was 4-fluorine benzene, the quantum yields of the compounds in the aggregation state could reach 10.9% and 12.6% with methoxy (**c33**) and *N,N*-diphenyl (**c34**) on R₂, respectively.

To better understand the AIE mechanism of these compounds, we selected the crystal structure of **c3** as an example to analyze the structure-function relationship. As illustrated in Fig. 2, **c3** displayed a propeller-like shape, the dihedral angle between the heterocycle plane and the benzoyl plane was measured to be 45.7° as well as a dihedral angle of 34.2° between the heterocycle and benzene plane. Therefore, the C–C single bond between the conjugate planes became highly rotatable in the dissolved state and cause energy loss through a series of non-radiative transitions, which would be weakened in the aggregation or solid-state, resulting in excellent AIE performance. Also, strong O–H interaction was also observed in molecular packing diagrams, which could also effectively restrain the intramolecular motions (Fig. 2b). To verify the effect of this special intramolecular hydrogen bond, a control experiment was conducted to compare the respective luminescence

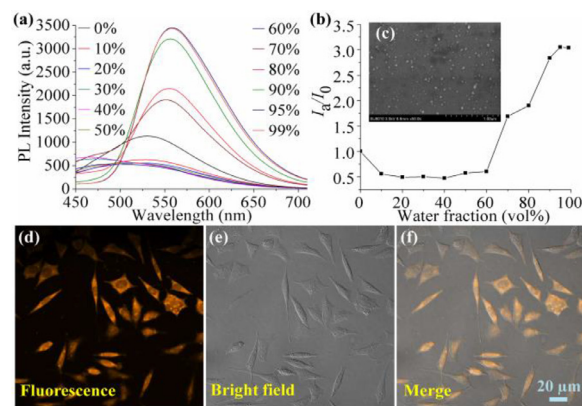


Fig. 3. (a) Fluorescent spectra of **c34**. (b) Emission spectra of **c34** in H₂O/THF solution. (c) SEM image of **c34** in H₂O/THF (99/1, v/v). (d) Fluorescent image of HeLa cells stained with **c34** (20 μmol) for 20 min. (e) The bright-field image of cells. (f) The overlaid image of d and e.

characteristics before and after the replacement of the nitrogen α -H on pyridine with chloride atom. As shown in Fig. 2c, **c3** solution (THF) exhibited a significant change in the maximum emission wavelength (485–510 nm) and quantum yield (2.9%–7.3%) when the water fraction was raised from 0% to 99%. In contrast, when the α -H was substituted by chloride (**c37**, Fig. S43 in Supporting information), although an obvious red-shift of the maximum wavelength could be observed, the fluorescence quantum yield did not change significantly. These results confirmed that the formation of O–H interaction indeed played an important role in promoting the AIE character.

To perform the biological imaging experiment, **c34** was chosen as a representative AIEgen due to the good AIE performance, the relevant long emission at 558 nm, and the highest quantum yield of 12.6% in the aggregation state among these obtained compounds (Figs. 3a and b). Moreover, the SEM image revealed **c34** would aggregate into spherical nanoparticles with a size range of 200–400 nm in the solution with high water content, which is suitable for biological applications (Fig. 3c). Furthermore, the MTT assay showed excellent viability of cells even when the concentration of **c34** reached 100 μmol/L (Fig. S44 in Supporting information). As illustrated in Figs. 3d–f, **c34** (20 μmol/L) showed efficient and ultrafast uptake by HeLa cell within 20 min and exhibited strong orange fluorescence signals in the cytoplasm, suggesting that **c34** could serve as a potential AIEgen for mapping important biological analytes in living cells.

Afterwards, the biological activity of the obtained compounds was investigated using **c27**–**c36** as examples beginning with virtual screening (Table S8 in Supporting information). To our delight, all the selected compounds exhibited high affinity for cannabinoid-2 (CB₂) receptor which is closely associated with inflammatory pathways [38,39]. Due to the lack of enough investigation of imidazo[1,5-*a*]pyrimidines derivatives upon the anti-inflammatory effect, we have chosen **c36** as the representative to assess the anti-inflammation activity via animal models (docking score of **c36** is better than **c35**). Then, arachidonic acid (AA) induced ear swelling test was performed to evaluate its anti-inflammatory effect (Fig. 4a). All the experimental protocols were approved by the Institutional Animal Experimental Ethics Committee of Northwest University (ethic code: NWU-AWC-20190202R). The results showed that **c36** could effectively prevent the ear swelling with an inhibition rate of 35.69% via intragastric administration (50 mg/kg), which is weaker than that of dexamethasone (**DEX**) (Fig. 4b). Moreover, **c36** could occupy a binding pocket mainly through hydrophobic interactions with the Phe87, Phe91, Ile110, Val113,

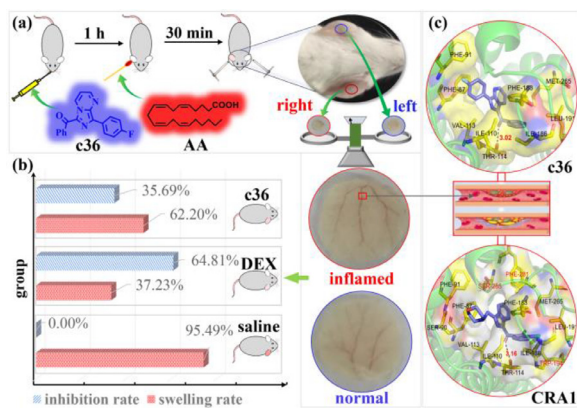


Fig. 4. (a) The arachidonic acid-induced ear swelling. (b) The activity of **c36** against the ear swelling. (c) The binding mode of **c36** and **CRA1** with CB_2 .

Thr114, Phe183, Ile186, Leu191, Met265 amino acids (Fig. 4c), which is consistent with the bind mode of reference CB_2 agonist **CRA1** [40]. These results indicated that **c36** could influence CB_2 's relevant anti-inflammatory signal path, and its modification is significant for the development of anti-inflammatory agents.

In summary, we have presented a series of twisted imidazo[1,5-*a*]pyridines via iodine-mediated Kornblum oxidation and cascade dual C–N bond coupling from phenylacetylenes or styrenes. Comparing with previous imidazo[1,5-*a*]pyridine based fluorophores, the optimized structures have overcome the adverse π – π stacking effect and enhanced the intermolecular rotation, leading to excellent AIE characters. The maximum emission could be easily modulated to achieve the desired performance to meet the requirement of bioimaging via regulating the electronic and steric effects. Moreover, compound **c36** was proven to be an anti-inflammation agent via the activation of the CB_2 receptor. This promising synthetic method will be beneficial to the development of new AIEgens and lead compounds.

Declaration of competing interest

The authors declare that they have no conflict of interests.

Acknowledgments

This work was financially supported by the National Natural Science Foundation of China (Nos. 22077099, 21807087 and 21673173), Key Research and Development Plan in Shaanxi Province of China (No. 2019KWZ-07), the Technology Innovation Leading Program of Shaanxi (No. 2020TG-031), the Xi'an City

Science and Technology Project (Nos. 2019218214GXRC018CG019-GXYD18.4 and 2020KJRC0115). We thank the support from COVID-19 Prophylaxis and Treatment Emergency Research Special Projects of Northwest University.

Supplementary materials

Supplementary material associated with this article can be found, in the online version, at doi:10.1016/j.ccl.2021.05.018.

References

- [1] J. Luo, Z. Xie, J.W.Y. Lam, et al., *Chem. Commun.* (2001) 1740–1741.
- [2] Q. Gao, L.H. Xiong, T. Han, et al., *J. Am. Chem. Soc.* 141 (2019) 14712–14719.
- [3] W. Chen, F. Song, *Chin. Chem. Lett.* 30 (2019) 1717–1730.
- [4] C. Wang, Z. Liu, M. Li, et al., *Chem. Sci.* 8 (2017) 3750–3758.
- [5] J.D. Zhang, Z. Yan, S. Wang, et al., *Dyes Pigm.* 150 (2018) 112–120.
- [6] D. Ding, G. Zhang, B.Z. Tang, L. Zheng, B. Situ, Patent, CN111239391 (A), 2020.
- [7] D.D. La, S.V. Bhosale, L.A. Jones, S.V. Bhosale, *ACS Appl. Mater. Interfaces* 10 (2018) 12189–12216.
- [8] J. Mei, N.L.C. Leung, R.T.K. Kwok, J.W.Y. Lam, B.Z. Tang, *Chem. Rev.* 115 (2015) 11718–11940.
- [9] Y. Zhang, Y. Wang, J. Wang, X.J. Liang, *Mater. Horiz.* 5 (2018) 799–812.
- [10] P. Shen, Z. Zhuang, Z. Zhao, B.Z. Tang, *J. Mater. Chem. C* 6 (2018) 11835–11852.
- [11] Y. Yu, J. Chen, S. Tan, et al., *J. Mater. Chem. C* 9 (2021) 888–893.
- [12] L. Zhang, Y.F. Wang, M. Li, Q.Y. Gao, C.F. Chen, *Chin. Chem. Lett.* 32 (2021) 740–744.
- [13] W. Chi, J. Chen, W. Liu, et al., *J. Am. Chem. Soc.* 142 (2020) 6777–6785.
- [14] S. Chen, H. Li, P. Hou, *Anal. Chim. Acta* 993 (2017) 63–70.
- [15] Y. Ge, R. Ji, S. Shen, X. Cao, F. Li, *Sens. Actuators B* 245 (2017) 875–881.
- [16] S.L. Shen, X.Q. Huang, X.H. Lin, X.Q. Cao, *Anal. Chim. Acta* 1052 (2019) 124–130.
- [17] H. Sheng, Y. Hu, Y. Zhou, et al., *Dyes Pigm.* 160 (2019) 48–57.
- [18] K. Tajima, N. Fukui, H. Shinokubo, *Org. Lett.* 21 (2019) 9516–9520.
- [19] K. Sun, X.L. Chen, S.J. Li, et al., *J. Org. Chem.* 83 (2018) 14419–14430.
- [20] M. Liu, S. Ma, M.Y. She, et al., *Chin. Chem. Lett.* 30 (2019) 1815–1824.
- [21] F. Shibahara, R. Sugiura, E. Yamaguchi, A. Kitagawa, T. Murai, *J. Org. Chem.* 74 (2009) 3566–3568.
- [22] Z. Xie, J. Peng, Q. Zhu, *Org. Chem. Front.* 3 (2016) 82–86.
- [23] S. Chuprakov, F.W. Hwang, V. Gevorgyan, *Angew. Chem. Int. Ed.* 46 (2007) 4757–4759.
- [24] A. Joshi, D.C. Mohan, S. Adimurthy, *J. Org. Chem.* 81 (2016) 9461–9469.
- [25] A. Joshi, D.C. Mohan, S. Adimurthy, *Org. Lett.* 18 (2016) 464–467.
- [26] H. Wang, W. Xu, Z. Wang, L. Yu, K. Xu, *J. Org. Chem.* 80 (2015) 2431–2435.
- [27] M. Li, Y. Xie, Y. Ye, et al., *Org. Lett.* 16 (2014) 6232–6235.
- [28] C.T. Feng, H.J. Wei, J. Li, Y. Peng, K. Xu, *Adv. Synth. Catal.* 360 (2018) 4726–4730.
- [29] P. Qian, Z. Zhou, K. Hu, et al., *Org. Lett.* 21 (2019) 6403–6407.
- [30] H. Wang, W. Xu, L. Xin, et al., *J. Org. Chem.* 81 (2016) 3681–3687.
- [31] P. Qian, Z. Yan, Z. Zhou, et al., *Org. Lett.* 20 (2018) 6359–6363.
- [32] Y.D. Wu, X. Geng, Q. Gao, et al., *Org. Chem. Front.* 3 (2016) 1430–1434.
- [33] H. Wu, X. Guo, C. Yu, et al., *Dyes Pigm.* 176 (2020) 108209.
- [34] Y. Zhang, B. He, J. Liu, et al., *Phys. Chem. Chem. Phys.* 20 (2018) 9922–9929.
- [35] M.Y. She, Z. Wang, T. Luo, et al., *Chem. Sci.* 9 (2018) 8065–8070.
- [36] M. Yang, J. Deng, H. Su, et al., *Mater. Chem. Front.* 5 (2021) 406–417.
- [37] J. Li, S. Zhang, H. Zou, *Org. Chem. Front.* 7 (2020) 1218–1223.
- [38] S. Han, J. Thatte, D.J. Buzard, et al., *J. Med. Chem.* 56 (2013) 8224–8256.
- [39] X. Li, T. Hua, K. Vemuri, et al., *Cell* 176 (2019) 459–467.
- [40] B.W. Trotter, K.K. Nand, C.S. Burgey, et al., *Bioorg. Med. Chem. Lett.* 21 (2011) 2354–2358.